Solar Energy Materials & Solar Cells 142 (2015) 116–122

Contents lists available at ScienceDirect

Solar Energy Materials & Solar Cells

journal homepage: www.elsevier.com/locate/solmat

Carrier-diffusion corrected J_0-analysis of charge carrier lifetime measurements for increased consistency

Achim Kimmerle [1], Johannes Greulich, Andreas Wolf

Fraunhofer Institute for Solar Energy Systems (ISE), Heidenhofstraße 2, 79110 Freiburg, Germany

ARTICLE INFO

Article history:
Received 16 April 2015
Received in revised form
10 June 2015
Accepted 23 June 2015
Available online 9 July 2015

Keywords:
Lifetime
Silicon
Band-gap narrowing
Dark saturation current
QSSPC

ABSTRACT

We investigate the origin of the apparently reduced recombination parameter J_0 of highly doped regions obtained from e.g. QSSPC lifetime measurements at high injection densities as well as the influence of recombination at bulk defects on the recently updated J_0-analysis of QSSPC measurements in the Sinton lifetime tester software. Using the example of crystalline silicon, we show that the frequently observed reduction and underestimation of J_0, which is strongly pronounced at high injection levels, originate from neglecting the finite carrier diffusion coefficient. This work presents an analysis taking into account the finite carrier diffusion coefficient and thus enabling to evaluate charge carrier lifetime data at high injection levels leading to strongly increased consistency of the determined J_0. Furthermore, we give a simple correction term for the recently published analysis leading to a total independence of a reasonably injection-independent Shockley–Read–Hall (SRH)-lifetime in the substrate. Combining the proposed methods, the determination of J_0 from numerically simulated lifetime-data is accurate within 3% of the input $J_0 = 100$ fA/cm^2 over an injection range of 10^{14}–$3 \cdot 10^{16}$ cm^{-3}. The application of the proposed method to measured data of crystalline silicon devices is in excellent agreement with the simulations and shows a strongly improved linearity and thus constant extracted J_0 compared to the former and recently published methods, which underestimate J_0 at high injection levels, nearly independently from doping type and -level of the substrate. The new and simple method is implemented in a spreadsheet calculator enabling fast and robust data evaluation similar to the Sinton lifetime tester software.

1. Introduction

The recombination parameter J_0 of highly doped regions (e.g. emitters and back-surface fields) is an important parameter to characterize doping techniques and processes for their application in solar cells as well as a central input parameter for solar cell simulation. The common way to obtain J_0 is the analysis of the effective excess-carrier recombination lifetime τ_{eff} of symmetrical samples measured with the Sinton Instruments WCT-120 lifetime tester [1], firstly introduced by Kane and Swanson [2]. Frequently a decrease of the apparent J_0 is observed for high injection densities. Such behavior has been predicted by Kane and Swanson [2] due to the non-uniformity of the injection density for samples with high surface recombination activity. Mäckel et al. [3] extensively studied the approximation made in the method of Kane et al. for a range of measurement conditions. They demonstrated that the approximation makes J_0 dependent on the excess minority carrier density. Comparison of measurement simulation for a wide range of J_0 demonstrated that, even in high-quality silicon, J_0 should be determined from the analytical solution as a function of excess minority carrier density including Shockley–Read–Hall recombination. Min et al. [4] proposed an approach to find the best fit range for the determination of J_0. Using numerical device simulations, they showed that J_0 should be extracted within a specific range of injection carriers. This specific range can be directly determined from the measurement of the effective lifetime by fitting it with a simple power curve. Thomson et al. [5] introduced a method to determine J_0 by numerically solving the carrier density profile so that the simulated average carrier density matches the measured one. This method avoids the errors made by the approximations in the method by Kane et al. and was demonstrated for samples with a wide range of J_0. However, it complicates the procedure by numerical simulations compared to the direct evaluation in the Sinton lifetime tester's software. Recently, an adaption of the Kane and Swanson method was implemented in the Sinton lifetime tester software [6,7] that accounts for injection dependent band-gap narrowing in the substrate and thus enables the compatibility with state-of-the-art numerical simulation tools. Although it leads to J_0 which is more independent from substrate doping and applied fit-range, it is not independent of the

E-mail address: achim.kimmerle@ise.fraunhofer.de (A. Kimmerle).
[1] Tel.: +49 761 4588 5046.

http://dx.doi.org/10.1016/j.solmat.2015.06.043
0927-0248/

influence of an injection-independent Shockley–Read–Hall (SRH)-lifetime τ_{SRH} in the substrate and still shows decreased J_0 for high injection densities $\Delta n > 7 \cdot 10^{15}\,\mathrm{cm}^{-3}$. In this work, we improve this analysis to be independent from constant τ_{SRH}.

Furthermore, we show that the underestimation of J_0 at high injection levels originates from neglecting the finite carrier diffusion coefficient and presents a corrected analysis method that enables fitting at high Δn, implies the same band-gap narrowing as the former method and is robust against the influence of a constant τ_{SRH} and substrate doping level and -type. The superiority of the new method is demonstrated on simulated and measured data sets.

2. Approach

2.1. Methods

One method to extract J_0 of highly doped regions on symmetrical samples from the effective surface recombination velocity S defined at the edge of the space charge region is differentiating the basic relation [8]

$$J_0 = S\frac{qn_{i,eff}^2}{N_{dop} + \Delta n}, \tag{1}$$

with respect to the injection density in the base substrate Δn, where $n_{i,eff}$ is the effective intrinsic carrier density, N_{dop} the base doping density, and q the elementary charge. This leads to

$$J_0 = q\frac{\mathrm{d}}{\mathrm{d}\Delta n}\left(n_{i,eff}^2 S\right). \tag{2}$$

In the standard analysis methods [2,6,7], S is calculated from the surface lifetime defined as [9]

$$\frac{1}{\tau_s} = \frac{1}{\tau_{eff}} - \frac{1}{\tau_{intr}} - \underbrace{\frac{1}{\tau_{SRH}}}_{\frac{1}{\tau_{bulk}}} = \frac{1}{\tau_{corr}} - \frac{1}{\tau_{SRH}} \tag{3}$$

by $S = W/(2\tau_s)$, with the wafer thickness W, the intrinsic lifetime resulting from Auger- and radiative recombination τ_{intr}, the resulting carrier lifetime in the substrate τ_{bulk}, and the Auger-corrected lifetime τ_{corr}. This is basically the assumption of uniform injection density Δn and leads to [2]

$$J_0 = \frac{qW}{2}\frac{\mathrm{d}}{\mathrm{d}\Delta n_{av}}\left(\frac{n_{i,eff}^2}{\tau_{corr}} - \frac{n_{i,eff}^2}{\tau_{SRH}}\right) \approx \frac{1}{2}qWn_i^2\frac{\mathrm{d}}{\mathrm{d}\Delta n_{av}}\frac{1}{\tau_{corr}}, \tag{4}$$

with the (experimentally accessible) injection density spatially averaged over the wafer thickness Δn_{av}. In the former analysis, $n_{i,eff}$ is assumed to be injection independent – assuming τ_{SRH} being injection independent as well, this leads to the well-known expression [2] on the right hand side of Eq. (4). This expression together with the applied $n_i = 8.6 \cdot 10^9\,\mathrm{cm}^{-3}$ and $\tau_{intr} = 1.66 \cdot 10^{-30}\Delta n^2\,\mathrm{cm}^6/\mathrm{s}$ in the lifetime-tester software is denoted as *former_method* in this work. Recently, a new method was implemented in the Sinton lifetime-tester software, taking into account an injection-dependent $n_{i,eff}$ [6,7] due to BGN in the base substrate [10] and applying an updated model for τ_{intr} [11] (here denoted as *uniform_injection*). However, this approach neglects $\mathrm{d}/\mathrm{d}\Delta n(n_{i,eff}^2/\tau_{SRH})$ in Eq. (4), which is valid for most FZ-Si samples, but might not be a valid assumption for Cz-Si samples if SRH recombination in the substrate is pronounced. Here, we propose an iterative procedure: in the first iterative step, J_0 is calculated from Eq. (4) by the assumption of $\tau_{SRH} = \infty$ in the injection-range used for the fit. Then τ_{SRH} in and outside of the fit-range is calculated by subtracting the calculated surface recombination from the measured recombination by [2]

$$\frac{1}{\tau_{SRH}} = \frac{1}{\tau_{corr}(\Delta n_{av})} - \frac{1}{\tau_s(J_0, \Delta n_{av})} = \frac{1}{\tau_{corr}(\Delta n_{av})} - \frac{2J_0}{n_{i,eff}^2(\Delta n_{av})}\frac{N_{dop} + \Delta n_{av}}{qW} \tag{5}$$

The obtained (injection-dependent) τ_{SRH} is averaged over the fit-range and in the second iterative step applied in Eq. (4) for the evaluation of a corrected J_0. Iterating this procedure leads to a convergence of τ_{SRH} and J_0 (here denoted as *uniform_injection_corr*) with the latter being independent from a constant contribution of τ_{SRH}.

Analyzing QSSPC-data with these methods, one frequently observes a decrease in the obtained apparent J_0 for $\Delta n > 7 \cdot 10^{15}\,\mathrm{cm}^{-3}$, which was recently reported [2,3]. As will be shown in the present work, the origin of this underestimation lies mainly in the finite carrier diffusion and therefore a decreased density of excess charge carriers at the edge of the highly doped region, not accounted for by assuming uniform injection. However, S can be calculated more exactly by solving the decay equation [12], which for symmetrical lifetime samples (transient case) reads

$$S = \alpha_0 D\,\tan\left(\frac{\alpha_0 W}{2}\right) \approx \frac{W}{2}\left[\tau_s - \frac{W^2}{D\,\pi^2}\right]^{-1}, \tag{6}$$

with the (ambipolar) diffusion coefficient of the injected carriers D. The right hand side is the approximation proposed by Sproul et al. [13] and applied in this work. For constant photogeneration and negligible bulk recombination, π^2 has to be replaced by 12 [14]. However, Sinton et al. [15] showed that the factor 12 only holds for extremely high diffusion length in the bulk of the wafer which is not given for the regarded case of high injection densities. Additionally, since the difference between π^2 and 12 seems minor compared with the remaining uncertainty of the method, e.g. regarding the uniformity of the generation rate and for reasons of simplicity, π^2 is applied in all cases. Together with Eqs. (1) and (2) this leads to

$$J_0 = \frac{qW}{2}\frac{\mathrm{d}}{\mathrm{d}\Delta n_{av}}\left(\frac{n_{i,eff}^2}{\tau_s - \frac{W^2}{D\pi^2}}\right). \tag{7}$$

To obtain the same robustness against an injection-independent contribution of τ_{SRH}, we apply the same iterative procedure as above using an analytical solution of Eq. (7) analogously to Eq. (5):

$$\frac{1}{\tau_{SRH}} = \frac{1}{\tau_{corr}(\Delta n_{av})} - \frac{1}{\tau_s(J_0, \Delta n_{av})} = \frac{1}{\tau_{corr}} - \frac{1}{\frac{W}{2}\frac{qn_{i,eff}^2(\Delta n_{av})}{J_0(N_{dop} + \Delta n_{av})} + \frac{W^2}{D\pi^2}}. \tag{8}$$

The iterative application of the averaged results of Eqs. (7) and (8) is denoted as *diffusion_corrected* in the following. The applied methods in this work are listed in Table 1.

The ambipolar diffusion coefficient D is calculated in this work applying the mobility model by Klaassen [17,18] as published by Schindler et al. [19] to [20]

$$D = \frac{k_B T}{q}\frac{\mu_n\mu_p(n + p)}{n\,\mu_n + p\,\mu_p}, \tag{9}$$

with μ_n and μ_p being the electron and hole mobilities, and n and p the electron and hole concentrations, respectively, under the assumption of local charge neutrality. The device temperature is denoted as T and k_B is the Boltzmann constant. The temperature for all calculation in this work is set to $T = 25\,^\circ\mathrm{C}$.

Table 1
J_0 evaluation methods applied in this work.

	Models	Central assumptions
Former_method	$n_i = 8.6 \cdot 10^9\ cm^{-3}$, $\tau_{intr} = 1.66 \cdot 10^{-30} \Delta n^2\ cm^6/s$	τ_{SRH} constant, uniform injection
Uniform_injection	BGN: Schenk [16], τ_{intr}: Richter [11]	τ_{SRH} infinite, n_i injection dependent, uniform injection
Uniform_injection_corr	BGN: Schenk [16], τ_{intr}: Richter [11]	τ_{SRH} constant, n_i injection dependent, uniform injection
Diffusion_corrected	BGN: Schenk [16], τ_{intr}: Richter [11], D: Klaassen [17,18]	τ_{SRH} constant, n_i injection dependent, carrier diffusion by Sproul [13]

The method *Diffusion_corrected* includes several approximations, where the details for the first can be found in Ref. [3]:

- The bulk lifetime is uniform throughout the device and does not change during the photoconductance decay, in particular is τ_b a function of Δn_{av}.
- For the calculation of J_0 from S, Eq. (2), a uniform carrier profile is assumed.
- S is approximated by Eq. (6), which has been obtained for transient carrier density decay (Ref. [12]).
- The data evaluation of the QSSPC as well as the evaluation of D assumes uniform injection density, in particular Δn_{av} throughout the device.
- τ_{SRH} is independent of Δn and approximated by an iterative method.

2.2. Experiment

Symmetrical lifetime samples (Czochralski-grown silicon material, $W = 200$–$230\ \mu m$) of different base-doping type and concentration are produced with alkaline textured surfaces, exposed to the same industrial-type $POCl_3$-diffusion (resulting in a sheet resistance of $\sim 90\ \Omega$/sq.) and SiN_x passivation procedure. The samples are analyzed in a Sinton WCT-120 lifetime tester in the center of the wafer applying the generalized measurement mode. The methods to determine J_0 are applied to these data sets. The fit range is assumed to be $(1–1.5) \cdot 10^{16}\ cm^{-3}$ which is very close to high injection for the lowly doped substrates. In order to estimate the bulk charge carrier lifetime, the passivation layer is wet-chemically removed; the highly doped region is removed in a KOH solution and passivated with a PECVD SiO_xN_y [21] stack. After activation of the passivation in a contact firing step with a set-temperature of 700 °C, the effective lifetime is evaluated with the same QSSPC setup.

2.3. Simulation

To compare the influence of the different evaluation methods, we create data sets of effective lifetime τ_{eff} over average injection density Δn_{av} for symmetrical lifetime samples by the simulation software QsCell 5.7 [22], which applies steady state conditions. We choose the implemented RG850-spectrum for excitation simulating the irradiation with the QSSPC flash lamp and the application of a RG850 red filter. We apply the $n_{i,eff}$ model that accounts for injection-dependent band-gap narrowing (BGN) in the substrate as the recently published method [7]. The software calculates Δn_{av} in the wafer by calculating an effective conductivity, very similar to the QSSPC measurement setup. Furthermore, τ_{eff} is calculated similar to the quasi-steady state mode of the QSSPC measurement. We then evaluate J_0 using the aforementioned methods by evaluating differentially the data of two successive illumination intensities.

3. Results

3.1. J_0-analysis

Fig. 1 shows the apparent J_0 differentially obtained for two successive measurement points over injection density Δn_{av} by the different methods. Additionally, the analysis results of the simulation data are shown. In the simulation, $J_0 = 208\ fA/cm^2$ is applied for all samples showing the best agreement for all samples and analysis methods, whereas for each sample an individual, but injection-independent τ_{SRH} is applied which was obtained by evaluating Eq. (8) on the measured data sets in the fit-range.

The simulated data sets are in excellent agreement with the measurement results for all wafers. The *former_method* underestimates J_0 in the chosen fit-range by up to 35% although at lower injection densities, lower deviations are observed. The method *uniform_injection* shows a significantly decreased deviation which can be attributed mainly to the considered BGN. The iterative correction for the finite τ_{SRH} visible by comparing *uniform_injection to uniform_injection_corr* has only minor influence of $\sim 8\ fA/cm^2$ for the substrate with the lowest $\tau_{SRH} = 180\ \mu s$. Still the deviation increases with injection density up to 17 % in the fit-range. In contrast, the method proposed in this work, *diffusion_corrected*, leads to apparent J_0 that are reasonably independent from the applied injection density, which is self-consistent and physically meaningful.

Fig. 2 shows the apparent J_0 obtained in the fit-range averaged for two wafers of each substrate doping. Since all wafers were subjected to the same texturization, diffusion and passivation processes, all samples are assumed to exhibit the same J_0. However, the *former_method* shows a large variation of the apparent J_0 with substrate doping. In this case, *uniform_injection* has no significant influence on this, showing an equally strong variation. In contrast, applying the *diffusion_corrected* method reproduces the expected independence of J_0 from the applied base substrate type and -doping. In addition, this method reproduces the input J_0 of the simulation very well.

Apart from this, the qualitative behavior of the apparent J_0 obtained from the different methods does not depend significantly on the applied base substrate or wafer thickness. Thus in the following, we exemplarily simulate a p-type substrate with specific resistivity $\rho_0 = 10\ \Omega\,cm$ and thickness $W = 200\ \mu m$.

To show the benefit of applying high injection densities, the analysis on simulation data of a symmetrical lifetime sample with $J_0 = 100\ fA/cm^2$ on each side and τ_{SRH} limited by recombination at non-cured boron-oxygen defect centers defined by $[O_i] = 5 \cdot 10^{17}\ cm^{-3}$ (parameterization implemented in QsCell 5.7 [22]) is shown in Fig. 3: following from Eq. (4), for lower injection densities the apparent J_0 is strongly influenced by the increasing injection dependence of τ_{SRH}^{-1}. Neglecting the finite diffusion coefficient (*former_method and uniform_injection*), the apparent J_0 decreases for higher injection densities leading to a maximum that is experimentally difficult to evaluate and still underestimates J_0 by 15% or 5% for the *former_method* or *uniform_injection*, respectively. Such behavior is in good agreement with the observations in the literature [2–5]. In contrast, the *diffusion_corrected* method enables a broad fit-range for $\Delta n_{av} > 7 \cdot 10^{15}\ cm^{-3}$ with a deviation below 3%, and 1.5% in the fit-range of $\Delta n_{av} = (1–2) \cdot 10^{16}\ cm^{-3}$.

The following simulations are analyzed in a fit-range of $\Delta n_{av} = (1–2) \cdot 10^{16}\ cm^{-3}$, which is very close to $10 \cdot N_{dop} \pm 30\%$ for

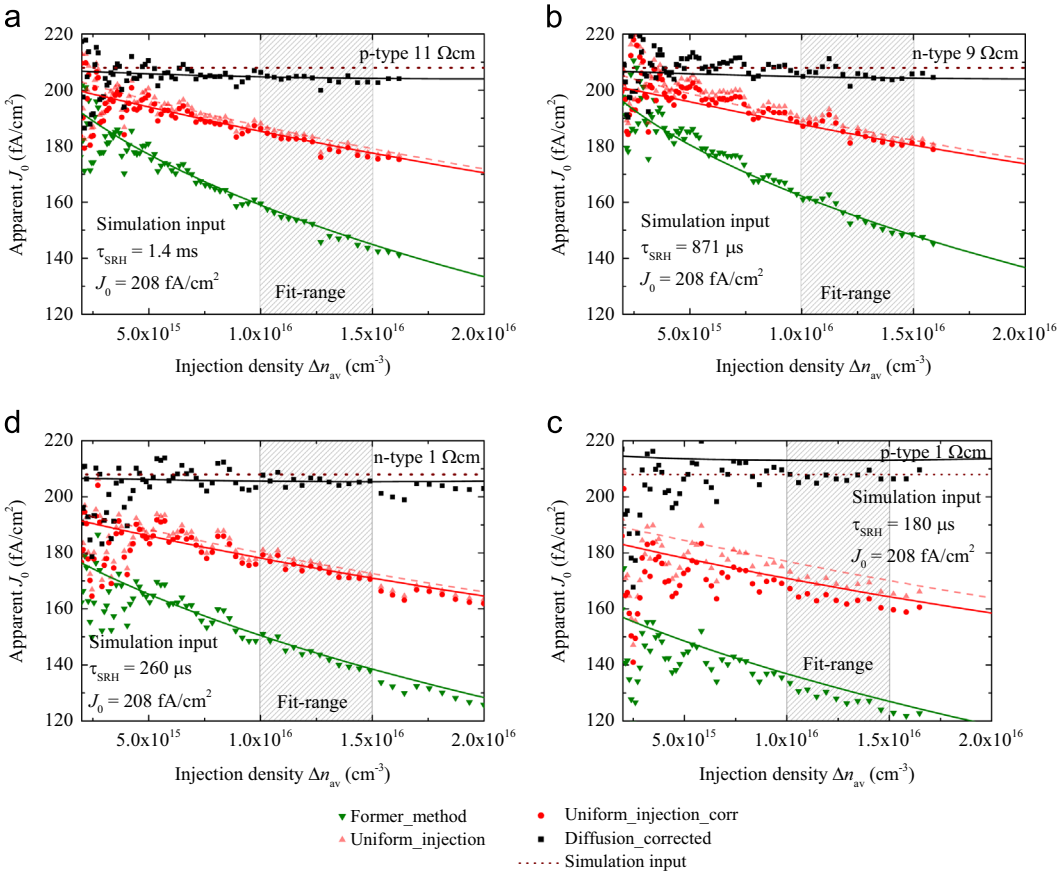

Fig. 1. Apparent J_0 over injection density Δn_{av} for the different applied base materials and methods. Each data point is the average of 3 neighboring apparent J_0 , each evaluated for two successive measurement points. In the simulation, $J_0 = 208$ fA/cm^2 is applied for all samples whereas a constant τ_{SRH} is applied resulting from averaging the result of Eq. (8) in the fit-range for each sample individually.

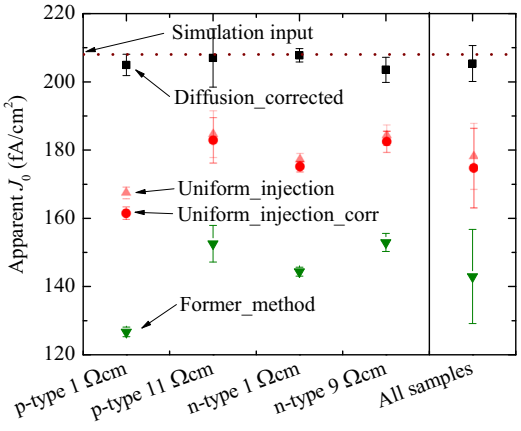

Fig. 2. Apparent J_0 after the different methods of each sample type evaluated in the fit-range $\Delta n_{av} = 10^{16}$–$1.5 \cdot 10^{16}$ cm^{-3}. Error bars denote the standard deviation of the point-wise evaluated data in the fit-range and of two samples for each base-substrate.

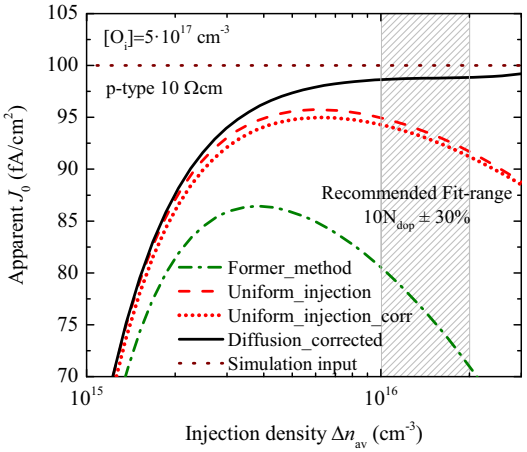

Fig. 3. Simulated apparent J_0 over injection density Δn_{av} of the different methods for a *p*-type 10 Ω cm substrate, applying an input value of $J_0 = 100$ fA/cm^2. For τ_{SRH}, the parameterization of recombination at boron–oxygen defects as implemented in QsCell [22], characterized by $[O_i] = 5 \cdot 10^{17}$ cm^{-3}, is chosen.

the applied *p*-type 10 Ωcm substrate. To evaluate the applicability of the analysis methods we simulate two different data sets: one with a constant $\tau_{SRH} = 500$ µs and varying J_0 (Fig. 4a) and one applying a constant $J_0 = 100$ fA/cm^2 and varying τ_{SRH} (Fig. 4b).

The *former_method* underestimates J_0 by more than 20% for all applied sets of input data (except for very low $\tau_{SRH} < 30$ µs which are not suited to extract the surface recombination). Considering BGN and updated models (*uniform_injection*) reduces the deviation by ~15% of the input J_0 . The iteration procedure to correct for τ_{SRH} is significant at $\tau_{SRH} = 500$ µs for $J_0 < 20$ fA/cm^2 (Fig. 4a) or at $J_0 = 100$ fA/cm^2 for $\tau_{SRH} < 100$ µs (Fig. 4b). The method *uniform_injection_corr* also shows an underestimation of the apparent J_0 of $> 10\%$ for $J_0 > 150$ fA/cm^2 due to the neglected carrier diffusion.

The *diffusion_corrected* method leads to similar results as *uniform_injection_corr* for $J_0 < 50$ fA/cm^2 where the diffusion towards the surfaces is apparently negligible. Both methods underestimate J_0 for very low input J_0 with a deviation of 10% at $J_0 = 4$ fA/cm^2.

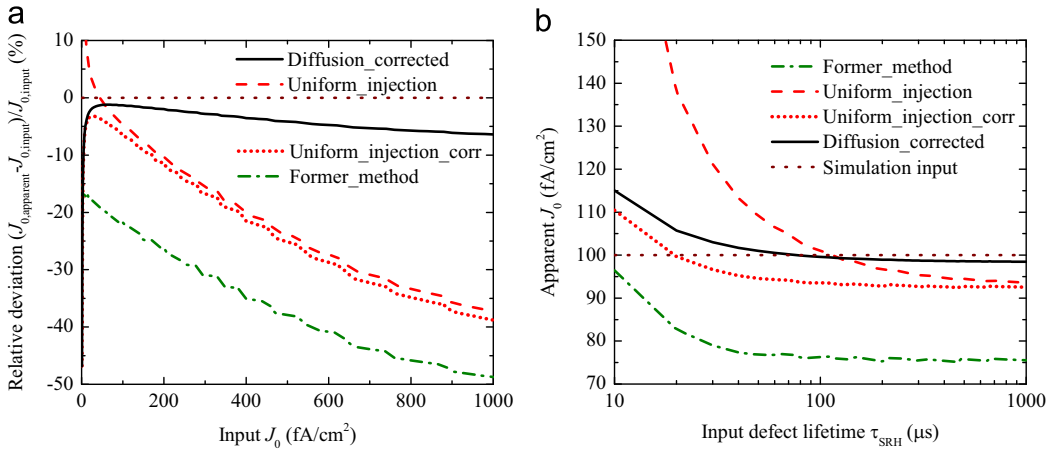

Fig. 4. Results from simulation data for *p*-type 10 Ωcm substrate of thickness W=200 µm analyzed with the different methods in a fit-range of $\Delta n_{av}=(1–2)\cdot 10^{16}$ cm^3. (a) Relative deviation of the apparent J_0 from the input J_0 assuming a constant τ_{SRH}=500 µs in the simulation. (b) Apparent J_0 assuming a constant input J_0=100 fA/cm^2 and different injection independent τ_{SRH}.

However, in this range the measurement results are dominated by experimental uncertainties.

Finally, the method *diffusion_corrected* shows a significantly reduced underestimation of J_0 , which is still below 7% for J_0=1000 fA/cm^2 (Fig. 4a) and for $\tau_{SRH}>20$ µs for J_0=100 fA/cm^2 (Fig. 4b).

3.2. Substrate lifetime

The evaluated J_0 , shown in Fig. 4, are applied to extract τ_{SRH} in the fit-range from the simulated data-sets using Eqs. (5) and (8). The results are shown in Fig. 5a for the variation of J_0 and Fig. 5b for the variation of τ_{SRH}, in correspondence to Fig. 4.

Since τ_{SRH} is calculated by subtracting the calculated surface recombination from the measured and Auger-corrected lifetime τ_{corr}, an underestimation of J_0 leads to an underestimation of τ_{SRH}. However, the higher the J_0, the more dominating the surface recombination and the higher the resulting uncertainty in τ_{SRH}. Consequently, the *former_method* underestimates τ_{SRH} by more than 10% for $J_0>17$ fA/cm^2 (Fig. 5a) or $\tau_{SRH}>90$ µs (Fig. 5b). The method *uniform_injection_corr* improves the reproduction of τ_{SRH} with a deviation of 10% at J_0=75 fA/cm^2 (Fig. 5a) or $\tau_{SRH}>210$ µs (Fig. 5b). Finally, diffusion_corrected leads to a deviation below 10% up to J_0=200 fA/cm^2 (Fig. 5a) and in the whole simulated range of $\tau_{SRH}<1$ ms (Fig. 5b). Note that all these values depend strongly on the applied fit-range, the applied J_0 and τ_{SRH}, and on the assumption of τ_{SRH} being sufficiently injection independent in the applied fit-range.

The same evaluation is taken out on the measured data-sets. Table 2 lists the analyzed τ_{SRH} by Eq. (8) (compare Fig. 1) and the corresponding measured τ_{corr} after removal of the highly doped region and re-passivation, both evaluated at $\Delta n_{av}=10^{15}$ cm^{-3}.

All analyzed τ_{SRH} are in agreement with the measured τ_{corr} of the passivated base-substrate.

4. Discussion

In the simulation and data-evaluation we apply the full Klaassen mobility model as adapted by Schindler et al. [23], taking into account lattice scattering, scattering at ions and free-carriers. Kane et al. [20] proposed to neglect free-carrier scattering when evaluating the ambipolar diffusion coefficient due to the parallel electron and hole particle flows. In contrast, Li and Thurber [24] showed that carrier scattering influences the carrier mobility even for carriers with the same average momentum, indicating that the injection density influences the carrier mobility even in the regarded lifetime samples.

Since the simulation and data-evaluation in this work apply identical models, the analysis of the simulated data-sets is not

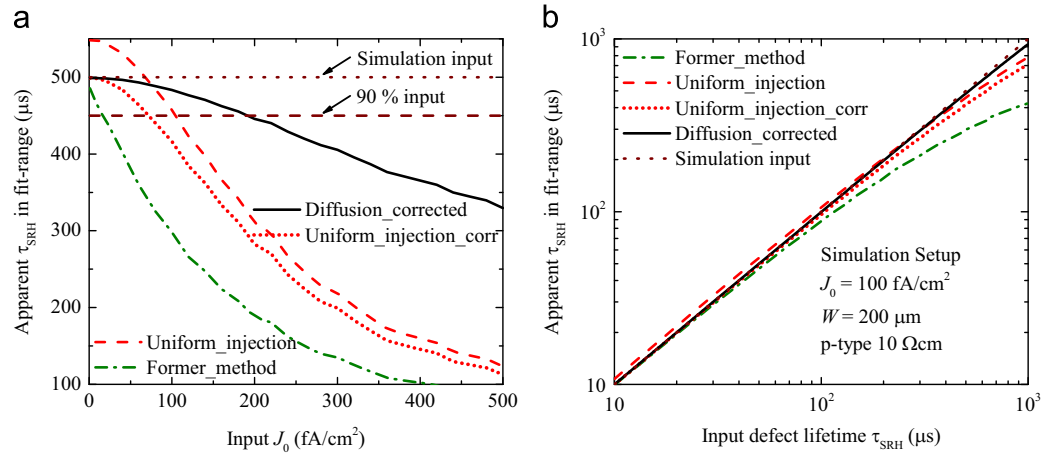

Fig. 5. Results from simulation data for p-type 10 Ω cm substrate of thickness W=200 µm analyzed with the different methods in a fit-range of $\Delta n_{av}=(1–2)\cdot 10^{16}$ cm^3. τ_{SRH} is calculated by applying the analyzed J_0 in the fit-range (see Fig. 4) in Eq. (5) or(8) according to the different methods and corresponding models. (a) Apparent τ_{SRH} over input J_0 assuming a constant τ_{SRH}=500 µs in the simulation. (b) Apparent τ_{SRH} assuming a constant input J_0=100 fA/cm^2 and different injection independent τ_{SRH}.

Table 2
Measured Auger-corrected lifetime τ_{corr} after removing the highly doped surface and passivation at $\Delta n_{av}=10^{15}$ cm^{-3}. And apparent τ_{SRH} obtained by Eq. (8), the apparent J_0 in the fit-range of $\Delta n_{av}=10^{16}$–$1.5\cdot10^{16}$ cm^{-3} (see Fig. 2) at $\Delta n_{av}=10^{15}$ cm^{-3}. Uncertainties denote an assumed 8% on the measured τ_{eff} and an additional uncertainty of 5% on the analyzed J_0.

	Phosphorus, 1 Ω cm, $N_D=5.3\cdot10^{15}$ cm^{-3}	Phosphorus, 9 Ω cm, $N_D=5.0\cdot10^{14}$ cm^{-3}	Boron, 1 Ω cm, $N_A=1.4\cdot10^{16}$ cm^{-3}	Boron, 11 Ω cm, $N_A=1.2\cdot10^{15}$ cm^{-3}
τ_{corr} measured after re-passivation (ms)	0.35 ± 0.03	1.0 ± 0.1	0.21 ± 0.02	1.0 ± 0.1
τ_{SRH} analyzed by Eq. (7) (ms)	0.36 ± 0.04	0.9 ± 0.1	0.17 ± 0.03	1.3 ± 0.3

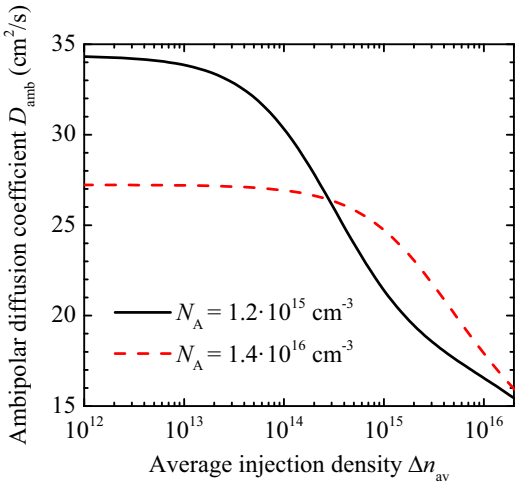

Fig. 6. Applied ambipolar diffusion coefficient for the simulation and analysis of the *p*-type samples (compare Fig. 1a and c).

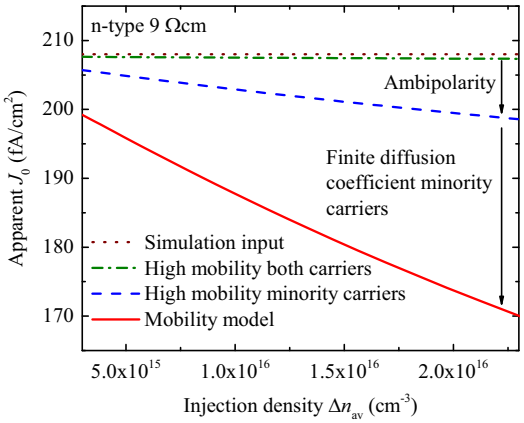

Fig. 7. Simulated apparent J_0 over injection density Δn_{av} of the method *uniform_injection_corr* for the *n*-type 9 Ωcm substrate (compare Fig. 1b). The numerical simulations either apply the mobility model, identical to Fig. 1b, an artificial high mobility for the minority carriers of 10^5 cm^2/Vs, or additionally an equally high mobility for the minority carriers.

affected by the choice of the mobility model. Moreover, the influence of the free-carrier scattering is estimated to be minor for the experimental data regarded in this work: the apparent J_0 obtained by Eq. (7) is reduced by approx. 1% for the measured samples when free-carrier scattering is turned off in the applied implementation of the carrier mobility. Fig. 6 shows the ambipolar diffusions coefficient after Eq. (9) over average injection density for the two *p*-type samples (compare Fig. 1a and c). The strong injection dependence in the range of the data-evaluation shows the necessity of applying an injection dependent ambipolar diffusion model.

The recently published method *uniform_injection* [6] shows increased reliability of the apparent J_0 for different substrates and applied doping densities due to consideration of plasma-induced BGN and the application of updated models. However, it is by construction not independent from the contribution of a constant τ_{SRH} in the fit-range. We propose an iterative correction, *uniform_injection_corr*, leading to the same independency from a reasonable injection independent τ_{SRH} as the *former_method*. The iteration converges typically after two steps and leads to no significant increase in computation time for the applied spread-sheet calculator.

The method *uniform_injection_corr* still shows significant underestimation of J_0 for high injection densities. Fig. 7 depicts the incrementally evaluated apparent J_0 , simulated for the *n*-type 9 Ω cm material shown in Fig. 1b. Three choices for the carrier mobility are made in the simulation: the mobility model applied in this work is used for both, minority and majority carriers (identical in Fig. 1b). The mobility of the minority carriers is artificially set to an unrealistic high value of 10^5 cm^2/Vs and, in a third simulation, the mobility of both carrier types is set to the same high value.

For high carrier mobility, the apparent J_0 corresponds within 0.3% to the input value for the whole range of simulated injection density. Applying Klaassen's mobility for the majority carriers leads to a decreased apparent J_0 of up to 5%. This decrease can be contributed to the ambipolar diffusion which limits the effective diffusion coefficient of the minority carriers to the diffusion coefficient of the majority carriers in high injection. Applying Klaassen's mobility for both types of carriers, similar to Fig. 1, the apparent J_0 decreases up to 29% in respect to the input value. The simulation confirms that the observed effect of the decreased apparent J_0 at high injection densities, obtained under the assumption of a homogeneous carrier profile, originates in the finite diffusion coefficient of the minority carriers in the base substrate. In particular, the recombination current at the surfaces is reduced because of the finite carrier flow towards the surfaces. We present a corrected analysis method, *diffusion_corrected*, applying the analytical correction of the surface lifetime proposed by Sproul et al. [13]. The method enables evaluating J_0 at high Δn and is robust against the influence of a constant τ_{SRH}. The application of the method is independent from doping type and -level of the substrate. It implies the band-gap narrowing model by Schenk [16] and the intrinsic lifetime by Richter [11] as the recently published method [6], the device simulator PC1Dmod [25] which is in very good agreement with Sentaurus Device [25], and the numerical emitter simulator EDNA [26]. The superiority of the new method is demonstrated on simulated and measured data sets. It enables reliable extraction of J_0 at high injection densities and thus the application of base materials with higher doping density or lower bulk carrier lifetime. It is implemented in a spread-sheet calculator in a very similar manner as the *former_method* and enables the same robust data evaluation with no significant increase in computation time.

Furthermore it is shown on measured and simulated data sets that the new method allows for the improved determination of τ_{SRH} in the base substrate of lifetime samples with diffused surfaces.

For the evaluation of J_0 , the *former_method* shows good reliability on lowly doped base material exhibiting high carrier lifetimes (e.g. FZ-Si) and thus enabling the data-evaluation at injection densities below $7 \cdot 10^{15}\,\mathrm{cm}^{-3}$. However, for the increased reliability, thus comparability of J_0-analysis on different base-substrates and injection densities, and the applicability in modern simulation tools, the authors recommend the presented method *diffusion_corrected* together with the application of a red-filter (RG850) for the extraction of J_0. For $J_0 < 100\,\mathrm{fA/cm}^2$ or injection densities below $7 \cdot 10^{15}\,\mathrm{cm}^{-3}$ the recently published method *uniform_injection* leads to very comparable results whereas for lower τ_{SRH} (e.g. Cz-Si) the method *uniform_injection_corr* should be applied. However, when τ_{SRH} is low, high injection densities are beneficial and thus the method *diffusion_corrected* seems recommendable in all cases.

5. Conclusion

Different methods to extract the recombination parameter J_0 of highly doped regions were evaluated and compared, based on measured and simulated charge carrier lifetime data. A new and simple method to determine J_0 at high injection conditions is proposed taking the finite carrier diffusion coefficient and Shockley–Read–Hall lifetime into account, which is particularly important for low bulk lifetimes and/or high recombination close to the wafer surfaces. This method shows results consistent with the experiment and reduces the commonly observed underestimation of J_0 significantly – to less than 7% for a wide range of bulk lifetimes and J_0. Additionally, the bulk lifetime at low injection conditions can be determined most accurately using this method with deviations of less than 10% for $J_0 \leq 200\,\mathrm{fA/cm}^2$ and $\tau_{SRH} < 1$ ms.

The presented evaluation method is implemented in a spreadsheet calculator and can be downloaded at www.sintoninstruments.com for the application on the measurement software of the Sinton lifetime tester.

Acknowledgment

This work has been supported in part by the German Federal Ministry for Environment, Nature Conservation and Nuclear Safety under Contract number 0325491 (THESSO). A. Kimmerle gratefully acknowledges the scholarship support from the Reiner Lemoine Stiftung. We thank Ron Sinton for fruitful discussions.

References

[1] R.A. Sinton, A. Cuevas, Contactless determination of current–voltage characteristics and minority-carrier lifetimes in semiconductors from quasi-steady-state photoconductance data, Appl. Phys. Lett. 69 (1996) 2510–2512.
[2] D.E. Kane, R.M. Swanson, Measurement of the emitter saturation current by a contactless photoconductivity decay method (silicon solar cells), in: Proceedings of the 18th IEEE Photovoltaic Specialists Conference, Las Vegas, Nevada, USA, 1985, pp. 578–583.
[3] H. Mäckel, K. Varner, On the determination of the emitter saturation current density from lifetime measurements of silicon devices, Prog. Photovolt.: Res. Appl. (2012) 1–17.
[4] B. Min, A. Dastgheib-Shirazi, P.P. Altermatt, H. Kurz, Accurate determination of the emitter saturation current density for industrial P-diffused emitters, in: Proceedings of the 29th European Photovoltaic Solar Energy Conference and Exhibition, Amsterdam, The Netherlands, 2014, pp. 463–466.
[5] A. Thomson, N. Grant, K.F. Chern, T. Kho, Improved diffused-region recombination-current pre-factor analysis, Energy Procedia 55 (2014) 141–148.
[6] A.L. Blum, J.S. Swirhun, R. Sinton, A. Kimmerle, An updated analysis to the WCT-120 QSSPC measurement system using advanced device physics, in: Proceedings of the 28th European Photovoltaic Solar Energy Conference and Exhibition, Paris, France, 2013, pp. 1521–1523.
[7] A. Kimmerle, P. Rothhardt, A. Wolf, R.A. Sinton, Increased reliability for J_0 -analysis by QSSPC, Energy Procedia 55 (2014) 101–106.
[8] A. Cuevas, M. Stocks, D. Macdonald, R. Sinton, Applications of the quasi-steady-state photoconductance technique, in: Proceedings of the 2nd World Conference on Photovoltaic Energy Conversion, Vienna, Austria, 1998.
[9] J.R. Haynes, W. Shockley, The mobility and life of injected holes and electrons in germanium, Phys. Rev. 81 (1951) 835–843.
[10] E.K. Banghart, J.L. Gray, Extension of the open-circuit voltage decay technique to include plasma-induced bandgap narrowing, IEEE Trans. Electron Dev. 39 (1992) 1108–1114.
[11] A. Richter, S.W. Glunz, F. Werner, J. Schmidt, A. Cuevas, Improved quantitative description of Auger recombination in crystalline silicon, Phys. Rev. B 86 (2012) 1–14.
[12] K.L. Luke, L.-J. Cheng, Analysis of the interaction of a laser pulse with a silicon wafer: determination of bulk lifetime and surface recombination velocity, J. Appl. Phys. 61 (1987) 2282–2293.
[13] A.B. Sproul, Dimensionless solution of the equation describing the effect of surface recombination on carrier decay in semiconductors, J. Appl. Phys. 76 (1994) 2851–2854.
[14] A. Cuevas, R.A. Sinton, Prediction of the open-circuit voltage of solar cells from the steady-state photoconductance, Prog. Photovolt.: Res. Appl. 5 (1997) 79–90.
[15] R.A. Sinton, H. Tathgar, S. Bowden, A. Cuevas, On the problem of determining the bulk lifetime of unpassivated silicon wafers, in: Proceedings of the 14th Workshop on Crystalline Silicon Solar Cells and Modules, Winter Park, Colorado, USA, 2004, pp. 1–4.
[16] A. Schenk, Finite-temperature full random-phase approximation model of band gap narrowing for silicon device simulation, J. Appl. Phys. 84 (1998) 3684–3695.
[17] D.B.M. Klaassen, A unified mobility model for device simulation. I. Model equations and concentration dependence, Solid-State Electron. 35 (1992) 953–959.
[18] D.B.M. Klaassen, A unified mobility model for device simulation – II. Temperature dependence of carrier mobility and lifetime, Solid-State Electron. 35 (1992) 961–967.
[19] F. Schindler, M.C. Schubert, A. Kimmerle, J. Broisch, S. Rein, W. Kwapil, W. Warta, Modeling majority carrier mobility in compensated crystalline silicon for solar cells, Sol. Energy Mater. Sol. Cells 106 (2012) 31–36.
[20] D. Kane, R. Swanson, Electron–hole collisions in concentrator solar cells, in: Photovoltaic Specialists Conference, 1988, Conference Record of the Twentieth IEEE, IEEE, 1988, pp. 512–517.
[21] J. Seiffe, L. Gautero, M. Hofmann, J. Rentsch, R. Preu, S. Weber, R.A. Eichel, Surface passivation of crystalline silicon by plasma-enhanced chemical vapor deposition double layers of silicon-rich silicon oxynitride and silicon nitride, J. Appl. Phys. 109 (2011) 034105.
[22] A. Cuevas, Modelling silicon characterisation, Energy Procedia 8 (2011) 94–99.
[23] F. Schindler, M. Forster, J. Broisch, J. Schön, J. Giesecke, S. Rein, W. Warta, M. C. Schubert, Towards a unified low-field model for carrier mobilities in crystalline silicon, Sol. Energy Mater. Sol. Cells 131 (2014) 92–99.
[24] S.S. Li, W.R. Thurber, The dopant density and temperature dependence of electron mobility and resistivity in n-type silicon, Solid-State Electron. 20 (1977) 609–616.
[25] H. Haug, A. Kimmerle, J. Greulich, A. Wolf, E.S. Marstein, Implementation of Fermi–Dirac statistics and advanced models in PC1D for precise simulations of silicon solar cells, Sol. Energy Mater. Sol. Cells 131 (2014) 30–36.
[26] K.R. McIntosh, P.P. Altermatt, A freeware 1d emitter model for silicon solar cells, in: Proceedings of the 35th IEEE Photovoltaic Specialists Conference, Honolulu, Hawaii, USA, 2010, pp. 1–6.